EREBUS

EuRopean Extinction BUmp Survey – Team Red

Team: *M. Bartylak, L. Capitanio, M. Cui, B. Engegaard, M. Gassner, S. Heinemann, S. Latzko, P.G. Madonia, A. May, A. Postel, J. Rodriguez Munoz, G. Schwarzkopf, R. Skalidis, V. Trivino Herrero, K. Wikman*
Tutors: *G. Kargl, R. Shipman*

Abstract

How does dust vary in size and composition throughout galaxies? The ultra-violet (UV) radiation can help us understand this. By comparing radiation from what we would expect a star to emit to what is observed, we can see how dust grains have "filtered" this light which hints at their size and composition. There are two dust features which appear at UV wavelengths, an extinction feature at 217.5 nm (the so-called UV bump) and a very sharp increase at the shortest wavelengths (the "far UV rise").
The EuRopean Extinction BUmp Survey (EREBUS) mission will map these features in our Milky Way Galaxy and the local group of galaxies and unveil changes in the dust carriers of both the UV bump and the far UV rise.

1 Science Goal

Mankind has always looked at the night sky in wonder and admiration. In the name of curiosity and in the spirit of adventure we have tracked the stars, studied the Sun and even walked on the moon. Our questions will forever remain the same. What is out there? Is there more than meets the eye? How does it all fit together in the grand puzzle that is our Universe? On of those things that doesn't meet the eye is the interstellar dust, or the ISM. It's a mix of dust and gas between the stars, and in this proposal we aim to describe a space mission designed to study this dust using a method involving something else that doesn't meet the eye - Ultraviolet light. By using spectroscopy to study how different wavelengths of the ultraviolet light is attenuated by the medium it passes through towards us we can learn a great deal about this medium.

Galaxy evolution is a not completely understood process. It is intimately linked with star formation as well as the interstellar medium (ISM). The ISM is the gas and dust between stars.
Observations reveal (e.g Planck Collaboration XI 2013) that dust is a ubiquitous component of the ISM. The dust that exists in the ISM is ultimately linked to the birth and death of stars. However, the composition and dynamic behaviour of this material is not fully understood. An important observational effect of the dust is the extinction of light passing through it. Cardelli et al. 1989 parameterized the wavelength dependence of the extinction ((1)). This extinction 'law' is shown in Figure 2.
The extinction curve reveals a significant absorption feature at 217,5 nm called the UV bump. This peak has a very constant central wavelength, but has a variable width. One can also find regions where the bump is absent (see Prévot et al. 1984). Hence, these variations are the touchstone that we have changes in the dust. The extinction 'law' is caused by dust grains of various sizes and composition which absorb and scatter the background light (Draine 2003).
The EuRopean Extinction BUmp Survey (EREBUS) will measure and map the UV bump and rise extinction features in the Milky Way galaxy and the local group of galaxies. The scientific objective of EREBUS is to investigate the large scale variations of the UV dust features in terms of the extinction it causes to starlight. EREBUS will explore all the known UV sources in the Milky Way up to a specific distance and in the local group. There are already 3D extinction maps based on infrared and optical measurements (Green et al. 2015, Capitanio et al. 2017). These maps reveal large scale variations in the grain dimensions on the galactic plane that are not apparently correlated with known galactic structures. By focusing on the far UV extinction, EREBUS will open a new window on interstellar dust. With our measurements, we can provide a three dimensional dust map of the extinction law in order to solve the puzzle of the contribution of dust in the galaxy evolution.

Recently, the laboratory identifications provide us with the particular kind of dust which causes this absorption: the *************************. (ADD CITATIONS)
The scientific objective for EREBUS is to understand what the large scale changes of the dust are, what the large scale evolution is and how they are correlated with the well-known stellar structures. Using the UV bump as a tool to measure the dust, we get the variation in composition, with the tails we know the dimensional and spatial variations.

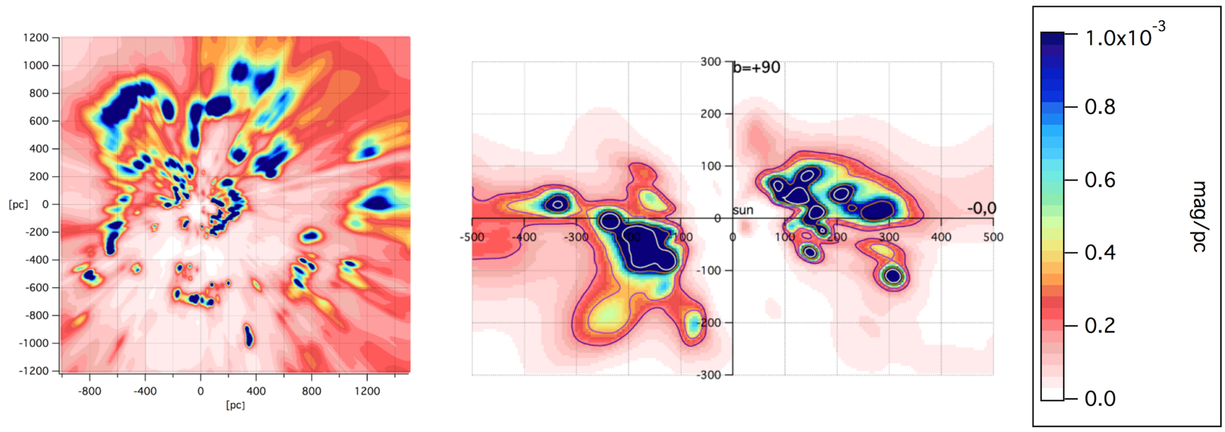

Figure 2: /textitleft: Extinction spectrum with the UV Bump shown; /textitmid,/textitright: Variation in the dimensional distribution of the dust .

This translates into our scientific goal as follows: We want to map the dust distribution in space, throughout the Milky Way in a 3-Dimensional structure and through the Local Group Galaxies in 2D.
There are 3D extinction maps based on infrared (IR) and optical measurements (Fig. **??**), but they cannot relate the measured changes with any particular kind of dust and they are based on the classical extinction law without taking in account any variations. There are some 2D maps of the spatial (FIGURE2) variability of dust based on the observations of the Planck satellite (ADD CITATION) - in IR emission and based on ground stationed observations - in IR extinction. The third dimension is missing in these observations and no correlation to the dust composition has been found.

With our measurements we can provide a dust map with the carbon composition and of all the others components present in the continuum of the extinction law. To achieve our goal we need a large UV survey of the Milky Way. we want to measure the UV spectra of thousand stars with known distances distributed throughout space. For each star we want to reconstruct the extinction law in the UV bump and its tails, so we need to have the stars spectrum in their spectral band. We compare the measured flux and the attended flux for every wavelength and reverse it to obtain the specific extinction law.
Then, with all the stars we can reconstruct the distribution in space. We can do that for each wavelength and measure the difference at large scales. We can also provide the deviation from the extinction law to understand what kind of structures and environments constrain the dust composition, evolution and behaviour.
Unfortunately, for the Local Group Galaxy we cannot measure the third dimension there because they are too far away, but we can map the changes in larger galactic regions. The strategy in this case is not to measure single stars, but the total emissivity and find the difference between what we attend - from galactic models - and what we obtain by our measurements to derive the extinction law. In this way we can measure the dust composition, evolution and behaviour in galaxies with different evolutionary histories, and provide a relationship between large scale dust structures and galactic history.

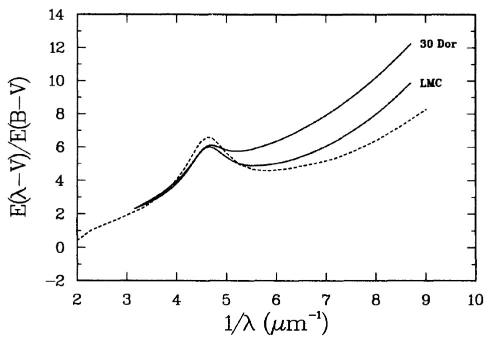

Figure 1: Ultraviolet extinction curves for the Large Magellanic Cloud (LMC), based on data from Fitzpatrick (1986). The average for stars widely distributed in the LMC (full curve) is compared with that for the 30 Doradus region of the LMC (broken curve) and the solar neighbourhood of the Milky Way

2 Science Objectives and Observational Requirements

Our scientific motivation is to understand the variation of dust in the Milky Way and other galaxies. To achieve that, we want to create a map of the dust variation in composition and grain size. We want to realise that using the extinction in UV in a systematic way. Observational requirement: measuring the properties of the UV extinction allover the sky including the feature at 217.5 nm, the so called "UV bump", in strength and width, as well as the shorter wavelength extinction, called "FUV rise".
To derive the extinction that occurs between stars or another bright source and us, we compare the observed light with the expected: the difference is the extinction. We want to measure this difference for various wavelengths between 100 nm and 300 nm.

To measure that difference, bright sources in UV are needed. In the Milky Way, there are the OB stars (temperature $\sim$ $40'000 - 10'000$ K, high temperature means blackbody emission peak in short wavelengths). Since the distribution of them is not homogeneously over the Galaxy, it is mandatory to consider also absorption for the A-stars (temperature $\sim$ $7'500 - 10'000$ K) which have photospheric UV emission, but also atomic stellar absorption features. To assign the appropriate theoretical emission model for the A-stars, we need to resolve spectral absorption in the order of 10 nm. In the Local Group galaxies, excepted for the Magellanic Clouds, we cannot resolve any single star, but we can observe the brighter star formation regions. We fixed as minimum requirement for our observation four points for each galaxy, and a single pointing for each OB star in star formation regions in the Milky Way. The different locations and difficulties in sense of measurement separate our targets into thre classes:

I. the O-B3 stars: those targets provide a very bright UV background, but they are not sufficient because of their diffuse spatial distribution in the sky and in distances. We have a catalogue fom SIMBAD of 5123 possible targets of that class.

II. the B3-A stars: they have less emission in the UV, but they are distributed also in the gaps of the O-B3 stars. We can provide 6026 possible targets in this class.

III. the brighter points in external galaxies: they have a diffuse emission, we cannot spatially resolve their position in their galaxy. We have 54 galaxies in our local group.

Scientific theme		Scientific sub theme		Scientific requirement		Observational requirement		Instrument requirement		Spacecraft requirement
Understand distribution and evolving behaviour of carbonaceous dust	S01	Understand distribution and evolving behaviour of carbonaceous dust in the Milky Way	SR01	Map stars in 3D	OR01	Identify differences in bump and wing in FUV with uncertainty < 0.1	IR01	Measure spectrum in 100 - 300 nm band	SC01	Internal temperature at 20 C, 1 C drift
	S02	Understand distribution and evolving behaviour of carbonaceous dust in other galaxies in the local group	SR02	Map stars in 2D	OR02	Observe >1 star in grid 10 degree square out to 5 kpc	IR02	Measure spectrum with resolving power > R = 300	SC02	Detector box temp at -100 C, 1 C drift
					OR03	Integrate for at least 5 hours	IR03	Measure photon count in each spectral bin from 120 - 300 nm with mean SNR > 10	SC03	Slew rate > 0.025 deg/s
					OR04	Identify differences in bump and wing in FUV with uncertainty < 0.1	IR04	No order overlap in spectrograph	SC04	Lifetime of essential systems > 5 years
					OR05	Observe >4 points for each galaxy in local group	IR05	Baffle	SC05	Support orbit to minimise airglow impact
							IR06	Detectors at -100 C, drift < 1 C	SC06	Support orbit outside of Van Allen belts
							IR07	Telescope structure at 20 C, drift below 1 C	SC07	Support orbit in low space debris density regime
							IR08	Calibration source		
							IR09	Shutter		
							IR10	Observe with angular resolution > 0.6 arcsec		

Figure 3: The Traceability Matrix.

3 Instrumental Requirements and Instrumentation

IRs: To observe a spectrum in the far UV (FUV) to medium UV (MUV), a spectograph is required and the observation location needs to be outside of the Earth's atmosphere, due to the well known opacity in this wavelength range. The instrument requirements (IRs) can be found in Table **??**.

3.1 Telescope

Our first requirement is the band to measure: 100-300 nm. Second requirement comes from the spectral absorption in photosphere of the A-stars, to resolve them we need an $lambda/\delta\lambda = 300$. To recognise variation in the extinction of 0.1 we need a SNR per beam of 10. To reconstrute the spectrum, our order shall not be overlapped.To measure different stars in the the sky without confusion we estimate an angular resolution < 0.6 arcsec.

The optical design chosen for the telescope is a Ritchey-Chretién configuration with a 35 cm primary mirror and a 4 cm secondary mirror. This design was chosen because it is commonly used and highly tested design for space telescopes.
We fixed the parameters for a first rough design, with a M1 focal lenght of $f_1 = 500$mm, and a distance of the focal plane from the primary mirror of 200 mm. Then an analysis and optimization was performed using a ray tracing software. The primary mirror was chosen as the aperture stop of the optical system.
This resulted in a final configuration with a 4 cm secondary mirror (M2), a working $f/\# = 19.7$ and a field of view of 0.8" " in order to have some margin in keeping the source within the FoV. The optimization process made possible to achieve diffraction-limited performances.
For the mirrors coatings we are using $Al{+}MgF_2$. This coating was chosen because it offers the best reflectivity ($\sim 85\%$) over our band of interest ($120 - 300$ nm). It is also flight-proven, does not suffer from degradation when exposed to atomic oxygen and offers low-but-usable reflectivity of at minimum 20% for the $100 - 120$ nm range.

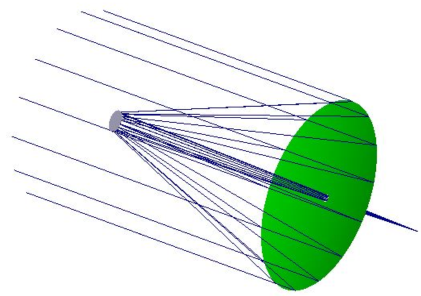

Figure 4: The Ritchey-Chretién Design of the Telescope.

3.2 Spectograph

The incoming light of the telescope has to be colimated before being dispersed. A common way to avoid unwanted overlap of different diffraction orders is to insert a second dispersive element in the beam path which's dispersion axis is rotated by 90° degree with respect to the dispersion axis of the first dispersive element. In that way, the higher diffraction orders of the first dispersive element will have a vertical offset from each other, thus a order overlap becomes impossible. After the gratings, the final mirror will focus the respective lines on the detector.
In general, the first grating is optimised for higher dispersion orders. However, for the EREBUS spectrograph, the order of interest is the first diffraction order, while higher orders will provide mainly a redundancy in our data and pixels, making the spectrograph more robust to disturbances or even pixel failure. Aiming for a high fidelity of the spectrograph our two dispersive elements will be realised by reflection gratings, since they have a higher efficiency than transmission gratings.

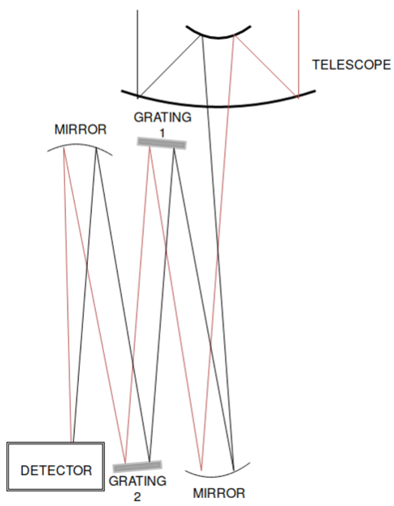

Figure 5: Schematic Design of the Spectograph.

3.3 Detector

The diffracted photons form a spectrogram on a Microchannel Plate Detector with a GaN photocathode. GaN is a relatively new photocathode material that was not yet flown into space. However it offers a vast improvement over the traditional technologies. GaN offers about 40% QE over $100 - 300$ nm, while otherwise we would have to use a combination of CsI and Cs_2Te limiting us to at most $\sim 30\%$ QE below 200 nm and $< 20\%$ for $200 - 300$ nm. MgF_2 window needs to be used to prevent degradation. Electrons emitted by the photocathode are subsequently amplified by MCP channels. The resulting electron cascade is then read by a detector (eg.

Charge Coupled Device (CCD) or a cross delay line (XDL) anode). The detector needs to be kept at 173 ± 1 K.

4 Spacecraft Design

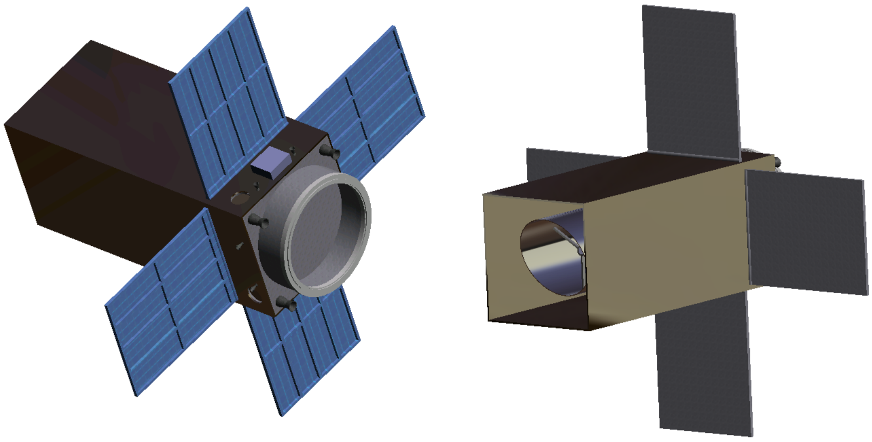

Figure 6: CAD Model of the Spacecraft. Dimensions 700x700x1700 mm

4.1 Size and Structure

After establishing the science baselines, the spacecraft design was developed to fulfil all the science requirements. In a first estimation, the observation time for the primary phase was calculated based on the apparent magnitudes in the U-Band of the stars in our catalogues. These were shifted to the 100-300 nm band and the incoming flux was derived, which was used to calculate exposure time estimates. Factors for observation efficiency, instrument efficiency, derivations from models and margins were used to correct this number.
To determine a first estimate for the aperture size, a cost calculation was made. We can determine the operational cost:

Operational cost [€] $\sim\ 2.613 \cdot 10^6 \cdot$ t[years]

From data of previous mission we can estimate a aperture size to satellite cost relation using the assumption that the aperture size is the driving design/size factor.

Satellite cost [€] $\sim\ 49 \cdot (d_{aperture}[cm])^{1.467}$

By combining these relations we derived a cost to aperture size diagram (Fig 8) which shows a minimum around $30-55$cm aperture diameter. This fits our limiting factor for the aperture size of ~ 40 cm because of production issues. The primary and secondary mirror are made of Zerodur due to its extremely low thermal expansion coefficient, low weight and proven flight heritage. An aperture of size of 35 cm was determined.
The quadrant sections around the propellant tank provide stiffness, while the baffles around the main payload section protect the instruments from being directly exposed to sunlight. Otherwise temperature and light variations could occur. Structures which could affect the mirrors positioning directly have all the same thermal expansion coefficient. The spacecraft's structures are made out of aluminium to avoid outgassing which could affect instruments.

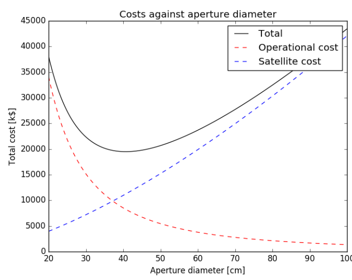

Figure 7: Cost to Aperture diameter

4.2 Orbit

Based on the science requirements the orbit should high enough to avoid the airglow from the earth atmosphere but still below the Van-Allen-Belt and to minimize the risk of space debris. From the engineering requirement a sun synchronous orbit was chosen to minimize the eclipse time. Other design considerations include thermal and power issues for the satellite and the easiest way to operate the satellite with ground stations.
We simulated the telescope de-orbiting time using STELA software. We decided to de-orbiting time the module in the circular orbit (550 km) to reduce de-orbiting time (23.41 years), ΔV required for de-orbiting is 311 ms^{-1}.
The maximum payload of Vega-C capability is 2300 kg in Low Earth Orbit (LEO). The launcher Vega performance in Sun Synchronous Orbit (SSO) at 1200 km is around 1000 kg. Thus a small satellite with 300 kg is

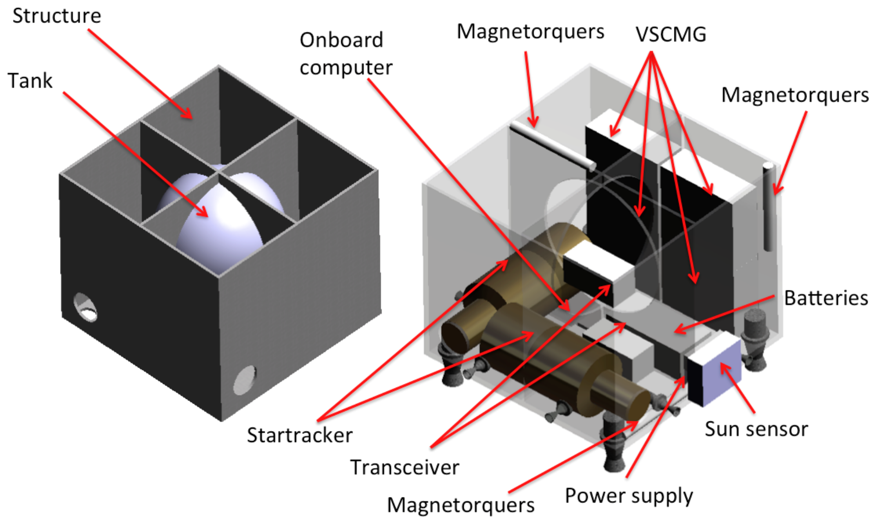

Figure 8: Left: Structure with the tank; Right: Internal components in the same Volume.

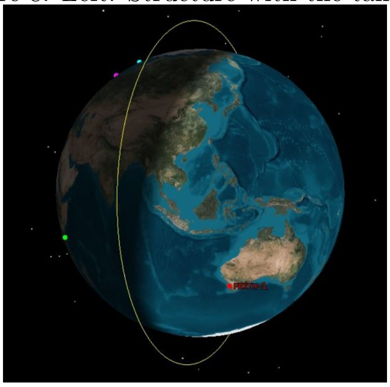

(a) Sun Synchronous Orbit

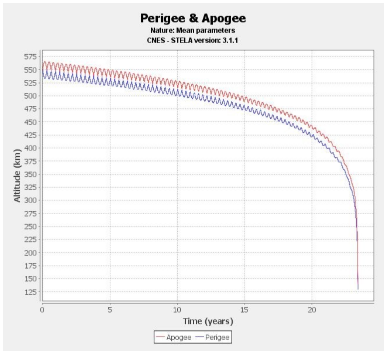

(b) De-orbit procedure

Figure 9: Orbit and De-orbit of EREBUS

launched with Vega-C. The launch is planned to take place in 2019. The direct transfer to the orbit is possible with the launcher.
Choosing the proximity of Kourou from the equator (latitude 5°) allowing a gain in performance (mass) for the launcher. The opening of Kourou on the sea allows a wide range of inclination for launching. Choosing an European launcher is a way to invest the money into the European market.

4.3 Thermal Design

4.4 Power

Assuming a solar flux of 1353 $\mathrm{W\,m^2}$ and accounting for the charging needs of the battery system, with the overall power demand of 300 W accounting for a 20% margin from the system power requirements, the solar array surface is 1.5 m^2.
The solar cells used on the array are IMM-α CIC Triple-junction InGaP/GaAs/InGaAs+InAs (QDs) and it is assumed a 25% efficiency (EOL) instead 30% efficiency (BOL) to take into account the power loses caused by degradation. This solar cells improve in efficiency (30%) compared to the commonly used cells 3J GaAs (27%). In addition the weight is reduced by half with respect to the same ones.
For energy storage an EnerSys ABSL Li-Ion battery with 40% of DoD cell array 8by8 with an oversized $E_{bat} = 278.4$ Wh and $C_bat = 12$ Ah is used to provide 28V to the DC bus of the PCDU and the power the system needs when the 34 min eclipses occur. To ensure a voltage of 28V on the DC bus a buck-boost DC/DC converter with a duty cycle of 0.5 is used.

4.5 Atitude Control, Stabilization and Pointing

To stabilize the spacecraft in space and to be able to reliably point and focus on the observation targets some specifiactions need to be made.
A stabilization control method of zero-momentum 3-axis will give us the highest accuracy compared to other

available methods. A star tracker as a main sensor gives the required pointing accuracy, and a Sun sensor is also available as a backup or to reorient the spacecraft if needed. To ensure the pointig stability,a technology based on FUSE heritage will be used.
Variable Speed Control Moment Gyroscopes (VSCMGs) will be used as the main attitude control actuators because they allow for fast and accurate changes in atitude. To desaturate the VSCMGs from momentum that builds up, magnetic torquers are used which avoid having to use propellant from the thrusters.
Thrusters are used both as a backup desaturation or attitude control method and for the end of life (EOL) manoeuvres.

	Required $\Delta V \mathrm{ms}^{-1}$
Orbit Injection Error Correction (3σ)	21
Orbit Keeping	60
Deorbiting	310
Desaturation of VSCMG	55
Total required ΔV	446

Table 1: ΔV Budget.

4.6 Onboard Computer, Data Handling and Telemetry

Data handling for all spacecrafts is an important feature to operate the spacecraft correctly and produce sufficient data for the scientific objective. For the EREBUS mission the data generated per day is estimated to be about, 2.3 MByte. The estimation is created under the assumption that the spacecraft will observe 300 objects per day (during normal operation the spacecraft will observe about 100 objects per day), an analog-to-digital converter of 16 bits, a data overhead of 64 bits and 30% extra bits for a safe margin. The amount of data per day is very low and will be no design driver.
All data is sent via telecommunications to ESA's ESTRACK ground stations on Earth. The Sun Synchronous Orbit will give a communication time with ground stations of about 928 seconds per day. The downlink speed of the system is 6.2 MB per second which will give approximately 5.8 GB per day, hence the spacecraft can transmit far more information than created by instruments . The communication operates at the S-Band at 2.2 GHz frequency.
Because the transfer rate and data created is small, the EREBUS spacecraft will use an off-the-shelf on-board computer, mass memory, command and data handling system provided by ÅAC Microtec(**?**). The processor used for the computer system is Leon3FT. The systems have been flown before on small satellites.

4.7 Operation Modes

During the mission lifetime the system will need to operate in different modes due to mission objectives, spacecraft disposal and spacecraft management. Due to this, the spacecraft got six different operation modes.

Mode	AOCS	Thermal	OBC	Communication	Payload	Safe AOCS
Launch and early life operation	X	√	√	√	X	√
Nominal	√	√	√	√	√	√
Safe	X	√	√	√	X	√
Orbit keeping	√	√	√	√	X	√
Eclipse	√	√	√	√	√	√
End of life	X	X	√	√	X	√

5 Mission Design

From the science objectives and the spacecraft design a mission time line can be derived.
The baselines were established using data from previous missions. For first phases we estimate $\sim$ 1 years each. With the progress the length of the phases increases and we estimate $\sim$ 2 years for these (Tab.

After the launch and and deployment, the operation phase starts. The EREBUS operation is divided into iterations. In the first iteration the coarse grid will be established which will then be refined by later iterations. One iteration phase is split into multiple observation phases.

6 Ground Segment

The data storage and distribution is handled through ESA's ESAC data center. The Data is processed and archieved to enable external access from the science community.

Budget Overview				
Subsystem	Mass Budget		Power Budget	
	Subsystem Margin [%]	Mass [kg]	Subsystem Margin [%]	Power [W]
Instrument	20	27.3	20	30
Power System	5	45.2	5	16.3
Launcher	5	1.1	5	0
AOCS	10	19.5	5	27.5
Structure	10	83.7	5	0
Thermal	5	3.2	5	58
Propulsion	10	18.5	5	86.1
Communication	5	6.6	5	3.2
OBDH/C&DH	5	5.8	5	6.9
	Nominal Dry Mass	211	Total Power	227.8
	Nom. Dry Mass +20% Marg.	253	Total Power +20% Marg.	273
	Satellite Wet Mass	298		

Table 2: Summary of the Mission Budgets.

Budget Overview	
Subsystem	Cost [mio €]
Launch	25
Payload	50
Service	40
Project Group	23
Operation	27.6
Total + Margin	108.72

Table 3: Summary of the Mission Budgets.

	Timeline [Years]							
Phases	2	4	6	8	10	12	14	......
Phase 0 needs indentification								
Phase A Feasibility								
Phase B Preliminary Definition								
Phase C Detailed Definition								
Phase D Qualification + Production								
Phase E Operation/Utilisation					Primary		Extended	
Phase F Disposal								

Table 4: Mission Project Phases

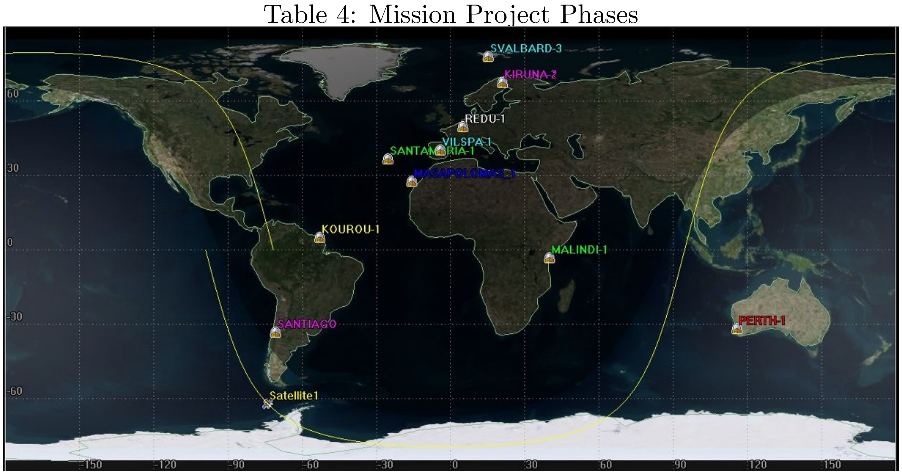

Figure 10: ESTRACK Ground Stations with an overlay of the Orbit.

7 Descope Options

Possible descope options require a reduction of the amount of targets observed. This could involve either reducing the size of our aperture (and therefore increasing the observation time per target) or simply reducing the duration of the mission. The catalogues of the possible targets could be refined to a minimum grid needed to have the required statistics.

8 Risk Mitigation

A space mission always bears some risks. The major risks that have been identified for the EREBUS mission are shown in Table 5. The risks were rated using the ESA risk assessment grades. The proposed risk mitigations are also shown.

Risk	Probability	Impact	Mitigation	Mit. Prob.	M. Impact
Exposure of instrument to bright sources (☉,♁,☽,..)	A	4	orbit, observation strategy	A	4
Calibration source mirror stuck in optical path	C	2	testing reliability ejection mechanism	B	1

Table 5: Risk Assessment

9 Public Outreach and Extended Mission Phase

The EREBUS mission lifetime is not limited by a specific component but rather by the continuous ageing process. We expect to be able to extend our mission from a technical point of view.

In the extended phase, secondary targets may be observed. These can include close Dwarf stars, T-Tauri stars and all OBA stars and galaxies that could not be observed in the primary mission phase.

We also propose a public outreach program to provide some observation time to the astronomical amateur community before we open to the science community.

10 Conclusion

EREBUS is where science meets engineering to change the way we look at the night sky. Our 3D map of how the extinction features in the UV are distributed in the Milky Way and our Local Group will provide extensive statistical data about the interstellar, and perhaps the intergalactic medium that could answer question about the abundance of carbonaceous materials, as well as information about dust properties. We cannot understand galaxy formation before we understand star formation, and we cannot understand star formation before we understand dust formation. Expanding our understanding of dust is what we aim to achieve. Our data will provide scientists and amateurs alike with important tools to take step forward in Humanity's quest of uncovering the secrets of our Universe. ((1),(2),(3),(4),(5),(6),(7),(8),(?),(?),(9))

References

[1] J. A. Cardelli, G. C. Clayton, and J. S. Mathis, “The relationship between infrared, optical, and ultraviolet extinction,” , vol. 345, pp. 245–256, Oct. 1989.

[2] A. A. Penzias and R. W. Wilson, “A Measurement of Excess Antenna Temperature at 4080 Mc/s.,” *Astrophysical Journal*, vol. 142, pp. 419–421, July 1965.

[3] J. C. Mather, E. Cheng, D. Cottingham, R. Eplee Jr, D. Fixsen, T. Hewagama, R. Isaacman, K. Jensen, S. Meyer, P. Noerdlinger, *et al.*, “Measurement of the cosmic microwave background spectrum by the COBE FIRAS instrument,” *The Astrophysical Journal*, vol. 420, pp. 439–444, 1994.

[4] M. Wenger, F. Ochsenbein, D. Egret, P. Dubois, F. Bonnarel, S. Borde, F. Genova, G. Jasniewicz, S. Laloë, S. Lesteven, and R. Monier, “The SIMBAD astronomical database. The CDS reference database for astronomical objects,” , vol. 143, pp. 9–22, Apr. 2000.

[5] B. T. Draine and J. C. Tan, “The Scattered X-Ray Halo around Nova Cygni 1992: Testing a Model for Interstellar Dust,” , vol. 594, pp. 347–362, Sept. 2003.

[6] G. M. Green, E. F. Schlafly, D. P. Finkbeiner, H.-W. Rix, N. Martin, W. Burgett, P. W. Draper, H. Flewelling, K. Hodapp, N. Kaiser, R. P. Kudritzki, E. Magnier, N. Metcalfe, P. Price, J. Tonry, and R. Wainscoat, “A Three-dimensional Map of Milky Way Dust,” , vol. 810, p. 25, Sept. 2015.

[7] E. L. Fitzpatrick and D. Massa, “An Analysis of the Shapes of Ultraviolet Extinction Curves. IV. Extinction without Standards,” , vol. 130, pp. 1127–1140, Sept. 2005.

[8] P. Collaboration, A. Abergel, P. Ade, N. Aghanim, M. Alves, G. Aniano, C. Armitage-Caplan, M. Arnaud, M. Ashdown, F. Atrio-Barandela, *et al.*, “Planck 2013 results. xi. all-sky model of thermal dust emission,” *A*, vol. 571, pp. A11–A11, 2013.

[9] M. L. Prevot, J. Lequeux, L. Prevot, E. Maurice, and B. Rocca-Volmerange, “The typical interstellar extinction in the Small Magellanic Cloud,” , vol. 132, pp. 389–392, Mar. 1984.